

High-pressure structural behaviour of nanocrystalline Ge

This article has been downloaded from IOPscience. Please scroll down to see the full text article.

2007 J. Phys.: Condens. Matter 19 156217

(<http://iopscience.iop.org/0953-8984/19/15/156217>)

View [the table of contents for this issue](#), or go to the [journal homepage](#) for more

Download details:

IP Address: 129.252.86.83

The article was downloaded on 28/05/2010 at 17:40

Please note that [terms and conditions apply](#).

High-pressure structural behaviour of nanocrystalline Ge

H Wang¹, J F Liu^{1,4}, Y He¹, Y Wang¹, W Chen¹, J Z Jiang^{1,4},
J Staun Olsen² and L Gerward³

¹ Laboratory of New-Structured Materials, Department of Materials Science and Engineering, Zhejiang University, Hangzhou 310027, People's Republic of China

² Niels Bohr Institute, Oersted Laboratory, University of Copenhagen, DK-2100 Copenhagen, Denmark

³ Department of Physics, Technical University of Denmark, DK-2800 Lyngby, Denmark

E-mail: nanoljf@zju.edu.cn and jiangjz@zju.edu.cn

Received 9 November 2006, in final form 21 February 2007

Published 26 March 2007

Online at stacks.iop.org/JPhysCM/19/156217

Abstract

The equation of state and the pressure of the I–II transition have been studied for nanocrystalline Ge using synchrotron x-ray diffraction. The bulk modulus and the transition pressure increase with decreasing particle size for both Ge-I and Ge-II, but the percentage volume collapse at the transition remains constant. Simplified models for the high-pressure structural behaviour are presented, based on the assumption that a large fraction of the atoms reside in grain boundary regions of the nanocrystalline material. The interface structure plays a significant role in affecting the transition pressure and the bulk modulus.

1. Introduction

The effect of finite crystallite size on the bulk modulus and on possible solid–solid phase transformations has been extensively investigated in order to improve our understanding of the structural stability and the mechanical properties of nanocrystalline materials. In their pioneering work, Tolbert and Alivisatos [1, 2] studied the wurtzite to rock salt structural transformation in CdSe nanocrystals. They showed that the transformation pressure increases with decreasing nanocrystal size. The change in transition pressure was explained in terms of differences in surface energies of the two phases. Indeed, the general rule seems to be the smaller the crystallites, the higher the transformation pressure, and several systems have been shown to behave accordingly, e.g. ZnO [3], ZnS [4], and PbS [5].

In contrast, Jiang *et al* [6] showed that the transition pressure for the γ to α transition in Fe₂O₃ is significantly lower for nanocrystals than for the bulk material. It was suggested that the large volume change at the transition and the existence of an unstable high-pressure phase

⁴ Authors to whom any correspondence should be addressed.

may lead to a reduction of the transition pressure in this particular nanocrystalline material. Since then, a similar behaviour has been observed for other systems as well, e.g. AlN [7], CeO₂ [8, 9] and the α to ε transformation in iron [10]. However, there are also systems, such as GaAs [11] and SnO₂ [12], for which the transition pressure is constant and independent of crystallite size. It follows from the above that competing processes determine the transition pressure, which can increase or decrease with decreasing crystallite size, depending on the system under investigation [13].

Similarly, the value of the bulk modulus has been found to decrease with decreasing grain size for Fe and Cu [14], Al₂O₃ [15, 16] and PbS [17]. On the other hand, the bulk modulus increases with decreasing grain size for nanocrystalline TiO₂ [18], CeO₂ [19], AlN [7], ZnS:Eu [20] and γ -Fe₂O₃ [6], whereas the bulk modulus of the nanocrystalline material is similar to that of the large-grained sample for Ni [21], ε -Fe [22] and CuO [23].

At ambient conditions, germanium crystallizes in the diamond-type structure with space group $Fd\bar{3}m$ (No. 227). This low-pressure phase is known as Ge-I. At about 10 GPa, germanium undergoes a semiconductor-to-metal transition. The high-pressure phase, Ge-II, has a tetragonal structure of β -Sn type with space group $I4_1/amd$ (No. 141). Bulk germanium at high pressure has been extensively studied, experimentally and theoretically; see [24–29] and more references in [30]. However, the high-pressure behaviour, in particular the structural stability, of nanocrystalline germanium is less known. The present work is an experimental study of the equation of state and the I–II transition of three germanium samples with volume-averaged crystallite sizes 13, 49 and 100 nm, respectively. Simplified models are presented to explain the observed high-pressure structural behaviour.

2. Experimental details

High-purity (99.999%) Ge was evaporated in helium atmosphere and condensed as a fine-grain powder on the surface of a cold finger. The material was stripped off and compacted in vacuum (10^{-3} Pa) by applying a uniaxial pressure of 1 GPa. The crystallite size was determined from the broadening of major x-ray diffraction peaks by applying the Scherrer formula. This gives the volume-averaged crystallite size. The size of the as-prepared crystallites was 13 nm. Samples with volume-averaged crystallite sizes of 49 and 100 nm were then obtained by annealing the as-prepared Ge pellets in vacuum at 473 K for 1 and 10 h, respectively.

High-pressure x-ray diffraction (XRD) spectra were recorded at the synchrotron-radiation facility HASYLAB in Hamburg, Germany. The diffractometer, operated in energy-dispersive mode, has been described elsewhere [31]. Pressures up to 35 GPa were obtained in a Syassen–Holzapfel-type diamond-anvil cell. The sample was placed in a 200 μ m diameter hole in an inconel gasket together with a ruby chip as a pressure marker. The actual pressure at the sample was measured by the ruby fluorescence method, using the nonlinear pressure scale of Mao *et al* [32]. A 16:3:1 methanol:ethanol:water mixture was used as the pressure-transmitting medium. The Bragg angle for each run was determined from a zero-pressure diffraction pattern of sodium chloride (NaCl).

3. Results and discussion

Figure 1 shows a series of energy-dispersive XRD spectra for 100 nm Ge at various pressures. The phase transition at about 10 GPa is clearly seen. For each spectrum, values of the lattice parameters and the unit-cell volume have been derived and refined by standard crystallographic techniques.

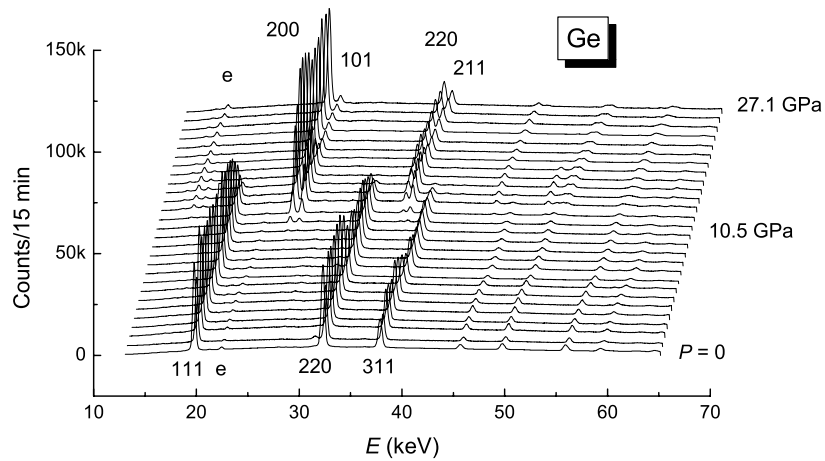


Figure 1. Energy dispersive x-ray diffraction spectra for 100 nm Ge with major reflections indexed; e = escape peaks due to the germanium detector. The phase transition above 10 GPa is clearly seen.

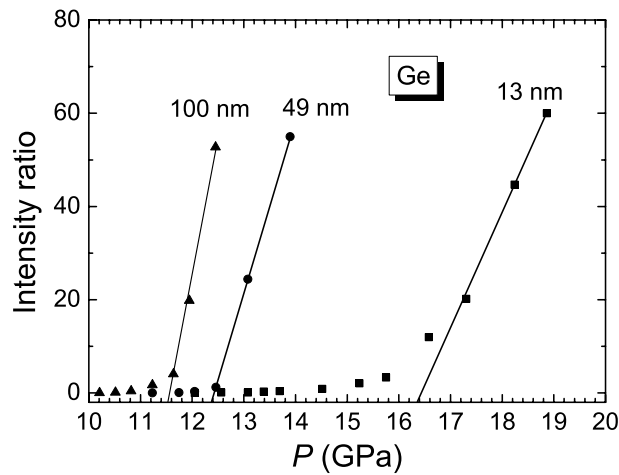


Figure 2. Transition pressures as determined by the extrapolation procedure (see text). The notation is as for figure 3.

In order to determine the transition pressure, P_{tr} , we have used an extrapolation method based on the ratio between diffracted intensities of selected high- and low-pressure peaks in the diffraction spectrum. This ratio is then plotted as a function of pressure, and the transition pressure is defined by extrapolation of the steep part of the curve to zero intensity (figure 2). We have found this procedure to be a fast and reproducible way of comparing transition pressures of different samples, and we have used it extensively in previous work [3, 6, 10, 11, 33]. In the present work, we have chosen to take the ratio between the intensities of the 200/101 doublet of Ge-II, and the sum of the 111 and 220 reflections of Ge-I (cf figure 1)

$$\frac{[I(200) + I(101)]_{Ge-II}}{[I(111) + I(220)]_{Ge-I}} \quad (1)$$

Table 1. Summary of experimental and theoretical results for Ge-I and the I \rightarrow II transition: a_0 is the lattice constant of Ge-I at ambient conditions, B_0 is the zero-pressure bulk modulus of Ge-I and B'_0 is its pressure derivative, P_{tr} is the transition pressure, and $-\Delta V/V$ is the magnitude of the volume collapse at the I \rightarrow II transition. The crystallite sizes given in the first column are volume-averaged values determined by the Scherrer formula.

Sample	a_0 (Å) expt.	B_0 (GPa) expt.	B'_0 expt.	B_0 (GPa) calc., model 1	B_0 (GPa) calc., model 2	P_{tr} (GPa) expt.	$-\Delta V/V$ (%) expt.	Ref.
Bulk	5.6576							[35]
Bulk		75						[36]
Bulk						8.0(5)	19.4(9)	[24]
Bulk						10.5(2)		[25]
Bulk		75(1)	3.0			10.6(1)	19.2(7)	[27]
100 nm	5.660(2)	88(3)	4.0			11.5(3)	17.5(3)	This work
49 nm	5.659(3)	92(3)	4.0	81.3	83.0	12.4(3)	17.3(3)	This work
13 nm	5.645(5)	112(5)	4.0	83.5	89.3	16.4(4)	17.3(4)	This work

The ratio defined by equation (1) is plotted in figure 2 as a function of pressure for the three crystallite sizes used in the present work. It is obvious that the transition pressure increases with decreasing crystallite size.

The unit-cell volume as a function of pressure, i.e. the compression curve, is plotted in figure 3(a) for the 100, 49 and 13 nm samples. It is seen that the phase transition in each case is accompanied by a volume collapse of about 17%. The compression curves for the low-pressure phase (figure 3(b)) can be described by the Birch–Murnaghan equation of state [34]:

$$P = \frac{3}{2}B_0(x^{-7/3} - x^{-5/3})[1 + \frac{3}{4}(B'_0 - 4)(x^{-2/3} - 1)], \quad (2)$$

where $x = V/V_0$, V is the volume at pressure P , V_0 is the volume at zero pressure, and B_0 and B'_0 are the isothermal bulk modulus and its pressure derivative, both parameters evaluated at zero pressure. The values of B_0 and B'_0 are obtained by a nonlinear least-squares fit of equation (2) to the experimental pressure–volume data points.

In table 1 we summarize our results for Ge-I and the I \rightarrow II transition and compare them with literature data. In order to facilitate the comparison of the B_0 values, we have followed the standard procedure of setting $B'_0 = 4.0$ for all samples. The bulk modulus and the transition pressure are seen to increase with decreasing crystallite size. In contrast, the lattice constant, a_0 , at ambient pressure is only slightly affected. Also the magnitude of the volume change, $-\Delta V/V$, at the phase transition is practically constant, about 17.3%, for all samples. Moreover, it is seen that the properties of the 100 and 49 nm samples are close to those of the bulk material, whereas the pressure behaviour of the 13 nm sample is markedly different. This is in good agreement with the findings of several authors that the effects of nanometre-sized crystallites become pronounced below a critical size, which is usually about 20 nm [37–39].

Figure 3(c) shows the compression curves for the high-pressure phase. Interestingly, it is seen that Ge-II mirrors the high-pressure behaviour of Ge-I as described above. Generally, the compressibility decreases (i.e. the bulk modulus increases) with decreasing particle size. Accordingly, the 100 nm sample is the most compressible one, but the 49 nm sample is only slightly less compressible than the 100 nm sample. In contrast, the compression curve for the 13 nm grain sizes shows that this sample is considerably less compressible than the 100 and 49 nm samples. Quantitatively, these findings can be expressed in terms of the bulk modulus, B_{tr} , evaluated at the transition pressure.

The bulk modulus, $B_{tr,I}$, of Ge-I, evaluated at the transition pressure, can be obtained by keeping only the first-order terms in the Maclaurin series:

$$B_{tr,I} = B_0 + B'_0 P_{tr}. \quad (3)$$

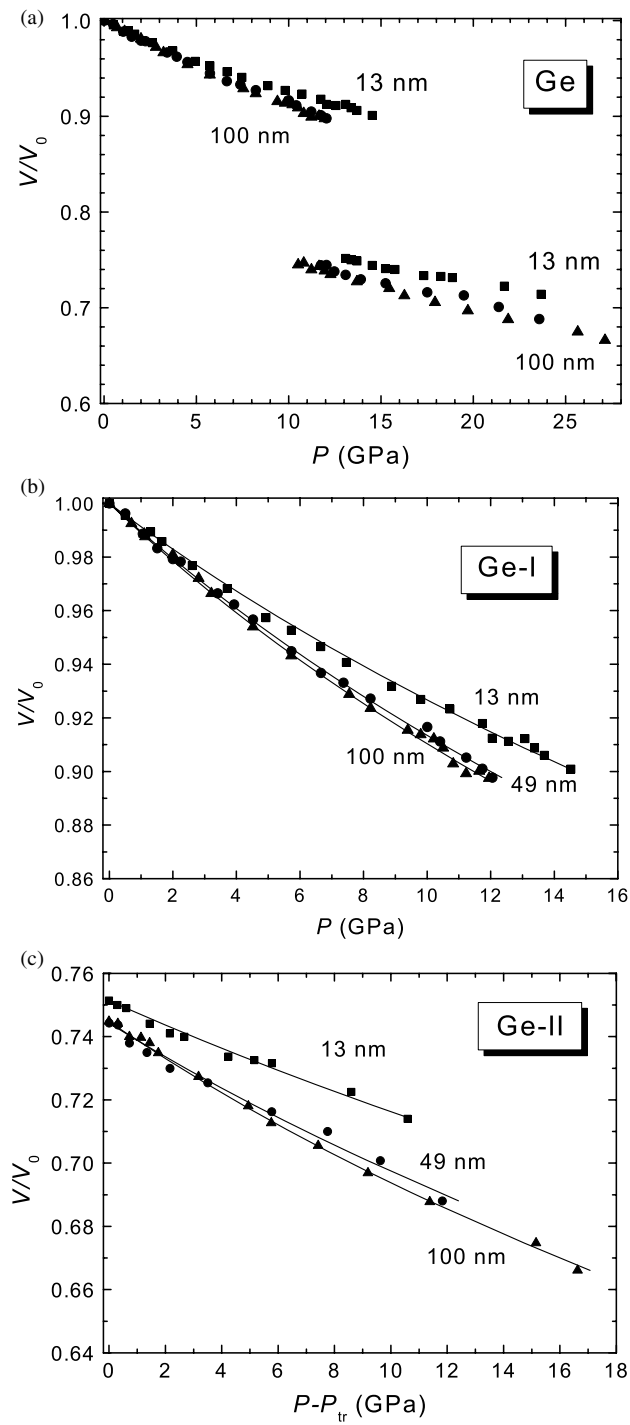


Figure 3. Compression curves. Filled triangles denote 100 nm, circles 49 nm, and square 13 nm particle sizes. Full curves are fits of the Birch–Murnaghan equation to the experimental pressure–volume data points. (a) Ge-I and Ge-II. (b) Ge-I. (c) Ge-II.

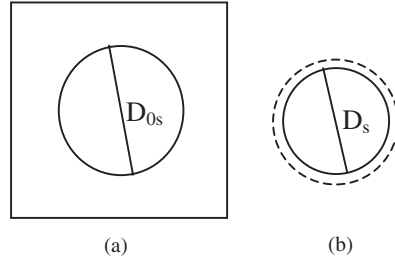


Figure 4. (a) A given spherical region with diameter D_{0s} in an infinite volume of material. (b) The corresponding nanometre-sized free particle with diameter D_s . The broken circle shows the diameter D_{0s} .

Table 2. Values of the bulk modulus, B_{tr} , and its pressure derivative, B'_{tr} , for Ge-I and Ge-II at the I \rightarrow II transition.

Sample	$B_{tr,I}$ (GPa)	$B_{tr,II}$ (GPa)	$B'_{tr,II}$	Ref.
Bulk	107(2)	90(7)	4.0(1)	[27]
100 nm	134(5)	120(5)	4.0	This work
49 nm	142(5)	135(5)	4.0	This work
13 nm	178(7)	190(7)	4.0	This work

For Ge-II, one can define a modified equation of state in terms of $(P - P_{tr})$, where P_{tr} is the transition pressure. Menoni *et al* [27] have described the procedure. Using a modified equation of Birch–Murnaghan type and nonlinear least-squares regression, we have determined the values of the bulk modulus $B_{tr,II}$ and its pressure derivative $B'_{tr,II}$, both parameters evaluated at P_{tr} .

Values of $B_{tr,I}$ and $B_{tr,II}$ are given in table 2 together with literature data for bulk Ge. It is seen that, for both phases, the values of the bulk modulus increase with decreasing crystallite size. Moreover, for given crystallite size and within the experimental error, the values of $B_{tr,I}$ and $B_{tr,II}$ agree. In other words, the two phases Ge-I and Ge-II are equally compressible at the transition pressure. This is also valid for bulk Ge, as seen in table 2.

In a simplified model, the bulk modulus and other elastic properties can be estimated from the Stillinger–Weber [40] two-body interatomic potential, u :

$$u = 2\varepsilon A \left[B \left(\frac{r}{\sigma} \right)^{-4} - 1 \right] \exp \left[\left(\frac{r}{\sigma} - 1.8 \right)^{-1} \right] \quad (4)$$

where r , the spacing of nearby atoms, is the one and only parameter determining u . Values of the parameters ε , σ , A and B for Ge are given by Ding and Andersen [41].

First, we will study the grain size effect on the surface energy. Consider a spherical region with diameter D_{0s} in an infinite volume of Ge with lattice parameter a_0 (figure 4(a)). It can be shown that the total potential energy of the sphere is given by

$$U_{0s} = 8 \frac{4\pi}{3} \frac{\left(\frac{D_{0s}}{2} \right)^3}{a_0^3} u_0 = \frac{4\pi}{3} \left(\frac{D_{0s}}{a_0} \right)^3 u_0 \quad (5)$$

where u_0 is the average potential energy per atom given by equation (4). If the sphere is separated from the surrounding matrix, the surface energy will induce a change in the potential energy and in the interatomic distance. As a result, the diameter of the sphere will change to D_s , as indicated in figure 4(b). For a nanometre-sized particle one can show that the following

Table 3. Surface energies of Ge-I and Ge-II, and numerical values of the terms which appear in equations (7) and (10).

Sample	Eqn.	Term 1 (GPa)	Term 2 (GPa)	Term 3 (GPa)	$\gamma_{\text{Ge-I}}$ (J m ⁻²)	$\gamma_{\text{Ge-II}}$ (J m ⁻²)
49 nm	(7)	0.14	0.99	-0.23	0.589	1.99
49 nm	(10)	0.14	1.10	-0.34	0.589	2.14
13 nm	(7)	0.23	6.14	-1.47	0.585	2.88
13 nm	(10)	0.23	5.69	-1.29	0.585	2.81

relation is valid:

$$\frac{1}{4}a_{0,n}^2\gamma_n = \frac{1}{4}a_{0,B}^2\gamma_B + \frac{D_n}{3a_{0,n}}(u_B - u_n) \quad (6)$$

where the subscripts B and n refer to bulk and nanocrystals, respectively. The surface energy is $\gamma_B = 589 \text{ mJ m}^{-2}$ for bulk Ge-I [42]. The corresponding energies, γ_n , for the 49 and 13 nm samples can now be calculated as 589 and 585 mJ m^{-2} , i.e. almost the same values as for the bulk material. Thus, grain size has only a minor influence on the magnitude of the surface energy of Ge-I.

It has been proposed that the effect of grain size on the transition pressure is governed by three factors: (i) the volume collapse at the transformation pressure, (ii) the surface-energy difference, and (iii) the internal-energy difference between the phases involved. The equation can be written as [13]

$$P_n - P_B = P_B \left(\frac{\Delta V_B(P_B)}{\Delta V_n(P_n)} - 1 \right) + \frac{U_{\text{nsurf}}(2, P_n) - U_{\text{nsurf}}(1, P_n)}{\Delta V_n(P_n)} + \frac{(U_B(1, P_B) - U_B(1, P_n)) - (U_B(2, P_B) - U_B(2, P_n))}{\Delta V_n(P_n)} \quad (7)$$

where the subscripts B and n refer to bulk and nanocrystals, respectively, P is the transition pressure, ΔV is the volume change at the transition, U is the internal energy of the core, and U_{nsurf} is the internal energy of the interface. The latter can be calculated as $U_{\text{nsurf}} = \gamma AN$, where γ is the average surface energy, A is the surface area of the crystal, and N is the number of the crystals per mole. The numbers 1 and 2 indicate Ge-I and Ge-II, respectively. The value of the last term of equation (7) can be found from the experimental pressure–volume data and the integral:

$$U_B(i, P_B) - U_B(i, P_n) = - \int P dV, \quad i = 1, 2. \quad (8)$$

The results of the calculations are listed in table 3. The experiments have shown that the volume collapse is practically independent of the grain size, cf table 1. Therefore, term 1 is small, as seen in table 3. Term 3 is found to be small and negative. It follows from term 2 that the surface-energy difference between Ge-I and Ge-II is the main factor determining the enhancement of the transition pressure.

The surface energy of Ge-II is found to be size dependent and about four times larger than that of Ge-I. The reason for this must be structural differences between the two phases with respect to the crystallite surfaces. It should be interesting to know the crystallographic orientation of the facets and the distribution of lattice defects at the crystallite surface. However, it has been impossible, at least for the moment, to make any microscopical analyses of the surface structure of the high-pressure phase. Upon release of pressure, the sample reverts to the low-pressure phase, and therefore *in situ* high-pressure studies, using for example electron

microscopy, would be necessary. To the best of our knowledge, no such studies have been reported in the literature.

In equation (7), the volume–pressure relationship is assumed to be similar for the bulk and nanophase materials. However, as shown in figure 2(b), the compressibility depends on the grain size. Thus, equation (8) needs to be modified as

$$U_B(k, P_B) - U_n(k, P_n) = U_B(k, P = 0) - \int_{P=0}^{P_B} P(k, B) dV \Big|_{P=0}^{P_B} - \left(U_n(k, P = 0) - \int_{P=0}^{P_n} P(k, n) dV \Big|_{P=0}^{P_n} \right); \quad k = 1, 2. \quad (9)$$

If the internal energies of bulk and nanocrystalline Ge at zero pressure, $U_B(k, P = 0)$ and $U_n(k, P = 0)$, are equal, then the revised version of equation (7) can be simplified as

$$P_n - P_B = P_B \left(\frac{\Delta V_B(P_B)}{\Delta V_n(P_n)} - 1 \right) + \frac{U_{\text{nsurf}}(2, P_n) - U_{\text{nsurf}}(1, P_n)}{\Delta V_n(P_n)} + \left[\left(\int_{P=0}^{P_n} P(1, n) dV \Big|_{P=0}^{P_n} - \int_{P=0}^{P_B} P(1, B) dV \Big|_{P=0}^{P_B} \right) - \left(\int_{P=0}^{P_n} P(2, n) dV \Big|_{P=0}^{P_n} - \int_{P=0}^{P_B} P(2, B) dV \Big|_{P=0}^{P_B} \right) \right] [\Delta V_n(P_n)]^{-1}. \quad (10)$$

The results of these calculations are summarized in table 2.

It should be noticed that the XRD signal originates from the coherent core region of the nanometre-sized grains. According to the two-component model devised by Gleiter [43], the nanocrystalline material consists of a crystalline component formed by the nanometre-sized crystallites and an intercrystalline component formed by the atoms in the boundary regions between the crystallites. Lattice parameters and unit-cell volumes estimated from the XRD measurements refer to the coherent regions of the grains. The bulk modulus in the present work is deduced from the pressure dependence of the unit-cell volume, which might be different from that of the true volume–pressure relationship for the sample.

Strain gradients are strong near the interfaces [44]. Thus, the lattice parameter might be varying in the grain, and the bulk moduli, obtained in the present work, should be considered volume-averaged values. The radius of the nanometre-sized particle corresponds to about 43 and 11 unit-cell lengths for the 49 and 13 nm grains, respectively. As mentioned above, there are no experimental studies of the distribution of lattice defects in the crystallites.

In order to make any predictions, at least qualitatively, we have considered two simplified models for the lattice parameter distribution in a grain: (1) the lattice parameter changes linearly from the core to the boundary, and (2) the lattice parameter is different in the outermost layer only, while it is the same as for bulk Ge in the interior of the grain. The latter model is essentially identical with the surface-shell–inner-core model, which was recently suggested by Palosz *et al* [45].

The first model suggests a compressive strain, $\Delta a/a$, which equals 5.5×10^{-6} for the 49 nm particles, and 3.1×10^{-4} for the 13 nm particles. In the second model, the lattice parameter in the outermost layer differs from the bulk value by $\Delta a = 0.01484 \text{ \AA}$ for the 49 nm particles, and 0.06280 \AA for the 13 nm particles. The values of the bulk modulus calculated from the two models are given in table 1. Both models agree with experiment in predicting that the bulk modulus increases with decreasing crystallite size. However, it is seen that the calculated values of the bulk modulus are consistently lower than the experimental values, probably due to oversimplifications in the models. It is most likely that the interatomic distance changes continually from the outermost layer to the core, but the interatomic distance and its gradient in

a small crystallite will also depend on the surface structure. More detailed knowledge would be required to have a better understanding of the grain-size effect on the bulk modulus and other elastic properties.

The bulk modulus is closely linked with the distance between neighbouring atoms in the crystal. In contrast to most other elements, Ge-I shrinks when it melts [46]. The structure of the grain-boundary regions are disordered, similar to a liquid. Thus, the density of these regions in Ge should be denser than in the crystalline material. This will cause a compression force on the core of the grain, resulting in a decrease of the lattice parameter, which is consistent with the experimental observations (table 1). Qualitatively, the compressibility of a grain should therefore decrease, i.e. the bulk modulus should increase, with decreasing grain size. More theoretical studies are needed, however, in order to make any quantitative predictions of the enhancement of the bulk modulus for nanocrystalline Ge.

4. Conclusions

We have studied the equation of state and the I–II transition of nanocrystalline germanium. It is found that the values of the bulk modulus and the transition pressure increase with decreasing particle size for both Ge-I and Ge-II. The effect is particularly large when the particle size is below a critical value of about 20 nm. Surface-energy differences between the phases involved can explain the increase of the transition pressure for the nanocrystalline material. Qualitatively, the enhancement of the bulk modulus can be attributed to compression effects due to the amorphous-like grain-boundary regions in the nanostructured material.

Acknowledgments

The authors would like to thank BSRF in Beijing and NSRL in Hefei, People's Republic of China; HASYLAB in Hamburg, Germany; and SPring8 and KEK in Japan for permission to use the synchrotron radiation facilities. We gratefully acknowledge financial support from the National Natural Science Foundation of China (Grant Nos 50341032 and 50425102), the Ministry of Science and Technology of China (Grant Nos 2004/249/37-14 and 2004/250/31-01A), the Ministry of Education of China (Grant Nos 2.005E+10 and 2005-55), Zhejiang University, and the Danish Natural Sciences Foundation through DANSYNC.

References

- [1] Tolbert S H and Alivisatos A P 1994 *Science* **265** 373
- [2] Tolbert S H and Alivisatos A P 1995 *J. Chem. Phys.* **102** 4642
- [3] Jiang J Z, Olsen J S, Gerward L, Frost D, Rubie D and Peyronneau J 2000 *Europhys. Lett.* **50** 48
- [4] Jiang J Z, Gerward L, Frost D, Secco R, Peyronneau J and Olsen J S 1999 *J. Appl. Phys.* **86** 6608
- [5] Jiang J Z, Gerward L, Secco R, Frost D, Olsen J S and Truckenbrodt J 2000 *J. Appl. Phys.* **87** 2658
- [6] Jiang J Z, Olsen J S, Gerward L and Morup S 1998 *Europhys. Lett.* **44** 620
- [7] Wang Z W, Tait K, Zhao Y S, Schiferl D and Zha C S 2004 *J. Phys. Chem. B* **108** 11506
- [8] Rekhi S, Saxena S K and Lazor P J 2001 *Appl. Phys.* **89** 2968
- [9] Wang Z, Saxena S K, Pischedda V, Liermann H P and Zha C S 2001 *Phys. Rev. B* **64** 012102
- [10] Jiang J Z, Olsen J S and Gerward L 2001 *Mater. Trans. (Japan)* **42** 1571
- [11] Jiang J Z, Olsen J S, Gerward L and Steenstrup S 2002 *High Pressure Res.* **22** 395
- [12] Jiang J Z, Gerward L and Olsen J S 2001 *Scr. Mater.* **44** 1983
- [13] Jiang J Z 2004 *J. Mater. Sci.* **39** 5103
- [14] Jiang J Z, Olsen J S, Gerward L and Morup S 1999 *Nanostruct. Mater.* **12** 847
- [15] Chen B, Penwell D, Benedetti L R, Jeanloz R and Kruger M B 2002 *Phys. Rev. B* **66** 144101
- [16] Zhao J, Hearne G R and Maaza M 2001 *J. Appl. Phys.* **90** 3280

- [17] Qadri S B, Yang J, Ratna B R, Skelton E F and Hu J Z 1996 *Appl. Phys. Lett.* **69** 2205
- [18] Swamy V, Dubrovinsky L S, Dubrovinskaia N A, Simionovici A S and Drakopoulos M 2003 *Solid State Commun.* **125** 111
- [19] Wang Z W, Zhao Y S, Schiferl D, Zha C S and Downs R T 2004 *Appl. Phys. Lett.* **85** 124
- [20] Pan Y W, Qu S C, Cui Q L, Zhang W W and Liu X Z 2001 *High Energy Phys. Nucl. Phys.* **25** 58 (in Chinese)
- [21] Rekh S, Saxena S K, Ahuja R, Johansson B and Hu J J 2001 *Mater. Sci.* **36** 4719
- [22] Chen B, Penwell D, Kruger M B, Yue A F and Fultz B 2001 *J. Appl. Phys.* **89** 4794
- [23] Wang Z W, Pischedda V, Saxena S K and Lazor P 2002 *Solid State Commun.* **121** 275
- [24] Baublitz M and Ruoff A L 1982 *J. Appl. Phys.* **53** 5669
- [25] Qadri S B, Skelton E F and Webb A W 1983 *J. Appl. Phys.* **54** 3609
- [26] Vohra Y K, Brister K E, Desgreniers S and Ruoff A L 1986 *Phys. Rev. Lett.* **56** 1944
- [27] Menoni C S, Hu J Z and Spain I L 1986 *Phys. Rev. B* **34** 362
- [28] Nelmes R J, Liu H, Belmonte S A, Loveday J S, McMahon M I, Allan D R, Häusermann D and Hanfland M 1996 *Phys. Rev. B* **53** R2907
- [29] Takemura K, Schwarz U, Syassen K, Hanfland M, Christensen N E, Novikov D L and Loa I 2000 *Phys. Rev. B* **62** R10603
- [30] Tonkov E Yu and Ponyatovski E G 2005 *Phase Transformations of Elements Under High Pressure* (Boca Raton, FL: CRC Press) pp 107–16
- [31] Olsen J S 1992 *Rev. Sci. Instrum.* **63** 1058
- [32] Mao H K, Xu J and Bell P M 1986 *J. Geophys. Res.* **91** 4673
- [33] Waskowska A, Gerward L, Olsen J S, Feliz M, Llusar R, Gracia L, Marqués M and Recio J M 2004 *J. Phys.: Condens. Matter* **16** 53
- [34] Birch F J 1938 *J. Appl. Phys.* **9** 279–88
Birch F J 1947 *Phys. Rev.* **71** 809
- [35] *Powder Diffraction File* PDF#5-545, International Center for Diffraction Data (ICDD), Newton Square, PA 19073-3273 USA
- [36] McSkimmin H J and Andreatch P 1963 *J. Appl. Phys.* **34** 651
- [37] Villain P, Goudeau P, Renault P O and Badawi K F 2002 *Appl. Phys. Lett.* **81** 4365
- [38] Shen T D, Koch C C, Tsui T Y and Pharr G M 1995 *J. Mater. Res.* **10** 2892
- [39] Zhou Y, Erb U, Aust K T and Palumbo G 2003 *Scr. Mater.* **48** 825
- [40] Stillinger F H and Weber T A 1985 *Phys. Rev. B* **31** 5262
- [41] Ding K J and Andersen H C 1986 *Phys. Rev. B* **34** 6987
- [42] Weast R C (ed) 1988–1989 *CRC Handbook of Chemistry and Physics* vol 69 (Boca Raton, FL: CRC Press) p F-23
- [43] Gleiter H 2000 *Acta. Mater.* **48** 1
- [44] Ke M, Hackney S A, Milligan W W and Aifantis A C 1995 *Nanostruct. Mater.* **5** 689
- [45] Palosz B, Stel'makh S, Grzanka E, Gierlotka S, Pielaszek R, Bismayer U, Werner S and Palosz W 2004 *J. Phys.: Condens. Matter* **16** S353
- [46] Glazov V M, Chizhevskaya S N and Glagoleva N N 1969 *Liquid Semiconductors (Monographs in Semiconductor Physics)* (New York: Plenum)